HHS Public Access

Author manuscript

Lab Invest. Author manuscript; available in PMC 2015 May 28.

Published in final edited form as:

Lab Invest. 2014 October ; 94(10): 1083–1091. doi:10.1038/labinvest.2014.95.

Differential effects of Akt1 signaling on short-*versus* long-term consequences of myocardial infarction and reperfusion injury

Lining Ma[1,2], **Bethany A Kerr**[1], **Sathyamangla V Naga Prasad**[1], **Tatiana V Byzova**[1], and **Payaningal R Somanath**[3,4]

[1]Department of Molecular Cardiology, Joseph J. Jacobs Center for Thrombosis and Vascular Biology, Lerner Research Institute, Cleveland Clinic, Cleveland, OH, USA

[2]Cardiovascular Department, Hainan Provincial People's Hospital, Hainan, China

[3]Clinical and Experimental Therapeutics, University of Georgia and Charlie Norwood VA Medical center, Augusta, GA, USA

[4]Department of Medicine, Vascular Biology Center and Cancer Center, Georgia Regents University, Augusta, GA, USA

Abstract

A specific role for Akt1 in events following myocardial infarction (MI) and ischemia/reperfusion (I/R) injury is not known. We aimed to determine whether Akt1 deletion in *in vivo* mouse models of MI and after ischemia I/R injury would alter myocyte survival, cardiac function, and fibrosis. $Akt1^{+/+}$ and $Akt1^{-/-}$ mice were subjected to MI and I/R, followed by assessment of downstream signaling events and functional consequences. Although no difference in infarct size following short-term MI was observed between $Akt1^{+/+}$ and $Akt1^{-/-}$ mice, I/R caused substantially more cardiomyocyte apoptosis and tissue damage in $Akt1^{-/-}$ mice compared with $Akt1^{+/+}$. Importantly, these effects were reversed upon pretreatment with GSK-3 inhibitor SB415286. Counterintuitively, $Akt1^{-/-}$ hearts exhibited improved cardiac function following long-term MI compared with $Akt1^{+/+}$ and were associated with reduced fibrosis in the left ventricle (LV). Our results demonstrate that Akt1-mediated inhibition of GSK-3 activity is critical for cardioprotection following I/R. However, in the long term, Akt1 contributes to fibrosis in post-MI hearts and might exacerbate cardiac dysfunction showing dichotomous role for Akt1 in cardiac remodeling after MI. Our data suggest that better understanding of the Akt1/GSK-3 pathway may provide insights for better therapeutic strategies in post-MI tissues.

Multiple signaling pathways downstream of Akt1 control cell survival, growth, metabolism, cell cycle progression, as well as motility of vascular cells.[1] We have previously reported that Akt1 is involved in the differential regulation of adaptive and pathological angiogenesis.[2,3] The importance of Akt1 in myocardial remodeling has been revealed using

Correspondence: Dr PR Somanath PhD, FAHA, Clinical and Experimental Therapeutics, College of Pharmacy, University of Georgia, HM1200 – Georgia Regents University, Augusta, GA 30912, USA. sshenoy@gru.edu.

DISCLOSURE/CONFLICT OF INTEREST

The authors declare no conflict of interest.

mouse models that overexpress constitutively active Akt1 (myrAkt1) in cardiomyocytes.[4–6] These mice exhibited pathological cardiac hypertrophy associated with a reduction in capillary density. Thus, Akt1 signaling might be involved in the regulation of several aspects of cardiac function and repair following an ischemic injury.

Glycogen synthase kinase-3 (GSK-3) is a major substrate downstream of Akt1 and its kinase activity is inhibited upon Akt1 activation. Similar to Akt1, the importance of GSK-3 in promoting myocardial remodeling has also been documented by studies utilizing mouse models that overexpress a constitutively active GSK-3β mutant.[7] In contrast to the existing paradigms, a recent study showed that although cardiomyocyte-specific conditional *GSK-3*$\beta^{-/-}$ mice exhibit normal hypertrophic response to pressure overload, long-term post-MI cardiac function is better preserved in these mice because of an improved remodeling process.[8] This indicates that consequences of constitutively active kinase mutant overexpression in mice are often off-target. Furthermore, a recent report demonstrated that knocking down GSK-3α in mice, another GSK-3 isoform in mammalian cells, results in impaired postischemic recovery in hearts.[9] This reciprocal regulation of postischemic cardiac remodeling by GSK-3α and GSK-3β indicates that more needs to be understood with regard to their regulation and contribution. Hence, utilizing *Akt1*$^{-/-}$ mice and a specific pan-inhibitor of GSK-3, we investigated the importance of this pathway in cardiomyocyte survival, cardiac remodeling, and output following myocardial infarction (MI) and ischemia/reperfusion (I/R) injury.

We hypothesized that disruption of the Akt1 gene will enhance cardiomyocyte apoptosis and interrupt cardiac remodeling. Here we demonstrate that Akt1 deficiency leads to apoptosis of cardiomyocytes and augments the cardiac damage immediately after reperfusion injury because of the activation of GSK-3β as well as destabilization of β-catenin. However, in the long term, it reduces fibrosis and improves cardiac function. Our study suggests that cotargeting Akt1 and GSK-3 may provide a beneficial effect on cardiac function and remodeling following cardiac insult.

MATERIALS AND METHODS

Reagents

Primary antibodies against phospho-GSK-3α/β Ser9/21, phospho-β-catenin, total β-catenin, total GSK-3β, Akt1, and pan Akt were purchased from Cell Signaling (Boston, MA, USA). CD31 antibody was purchased from BD Pharmigen. Masson's trichrome dye, 2,3,5-triphenyltetrazolium chloride and antibodies against α-SMA and β-actin were purchased from Sigma. All western blotting secondary antibodies were obtained from Bio-Rad (Hercules, CA, USA). Alexa Fluor-labeled secondary antibodies were purchased from Invitrogen (Carlsbad, CA, USA). Vectashield mounting media with DAPI were purchased from Vector Laboratories. GSK-3 inhibitor (SB415286) was obtained from EMD Biosciences (CA, USA). All other chemicals were purchased from Fisher Scientific.

Animals

We used age- and sex-matched *Akt1*$^{+/+}$ and *Akt1*$^{-/-}$ mice on the C57BL/6 background[2] at the ages of 8–10 weeks to perform coronary artery occlusion and reperfusion. All studies were reviewed and approved by the Institutional Animal Care and Use Committee at the Cleveland Clinic, Cleveland, OH, USA (Protocol no. ARC 08599).

Mouse MI and I/R Protocol

Mice were subjected to MI under general anesthesia (keta-mine 128 mg/kg and Xylazine 12.8 mg/kg) using surgical ligation of the mid left anterior descending (LAD) coronary artery according to the published protocol.[10] Mice were, in a supine position, intubated and mechanically ventilated using a rodent ventilator (model 683, Harvard, South Natick, MA, USA). Hair was removed from the left thoracic wall and cleaned with 75% alcohol. The chest was opened by a lateral incision along the upper margin of the fourth rib, muscles were transected, and hearts were exposed with retractor. Ligation was performed using an 8.0 silk suture, and a tapered needle was passed under the LAD coronary artery branch; a 1-mm section of PE-10 tubing was placed on top of the vessel, and a knot was tied in the tubing vessel to occlude the coronary artery. For the complete occlusion experiments, the knot was tied without PE-10 tubing. A dose of lidocaine (6 mg/kg) was then given intra-peritoneally. After 30 min of ischemia, the knot was cut in the PE-10 tubing to establish reperfusion. The chest wall was then closed, and the animal was removed from the ventilator and kept warm by bulb. The GSK-3 inhibitor SB415286 that inhibits both GSK-3α and GSK-3β isoforms was administered 5 min before reperfusion at a dose of 1 mg/kg body weight.[11]

Assessment of Infarct Size

The area at risk and infarct size was determined 24 h after MI (permanent occlusion) and after reperfusion. The chest was cut open, and the LAD coronary artery was reoccluded (for reperfusion model) through the previous ligation site. The aorta was cannulated using a section of PE-10 tubing, and 1% Evan's blue dye was perfused retrograde into the aorta and coronary artery system to allow distribution throughout the ventricular wall proximal to the coronary artery ligature to demarcate the ischemic area at risk. The nonischemic area was stained blue. The left ventricle (LV) was excised and sliced into five ~1 mm cross-sections below the ligature. Sections were then incubated in 1.5% 2,3,5-triphenyltetrazolium chloride (TTC) (Sigma) at 37 °C for 15 min. After the procedures, viable myocardium was stained red and the infarct appears pale. Images were taken using a microscope equipped with a digital camera. The infarct area (pale), the area at risk (not blue), and the total LV from both sides of each section were measured using Image-Pro software. The ratio of area at risk to LV and the ratio of infarct area to area at risk were calculated and expressed as percentages.

For histological analysis, hearts were collected rapidly and fixed in conventional fixing solutions (10% buffered formalin) after 30 min of left coronary artery ischemia and 14 days after reperfusion. Hearts were cross-sectioned into 1-mm-thick slices using a tissue chopper. Hearts were embedded in a standard manner and stained with hematoxylin and eosin. Digital images of the slides were captured and analyzed in a blinded manner using Image-Pro software to measure the area of infarct or scar relative to the LV. For each heart, four

sections taken from each 1-mm-thick slice were analyzed and averaged to obtain the size of the infarct or scar per LV for each animal.

Histological Assessment of Apoptosis and Fibrosis

For the apoptosis assay, animals were killed at 24 h after MI; hearts were removed and snap frozen. Transverse cryosections were cut at a thickness of 10 μm on a Leica Cryostatat and placed on superfrost plus-coated slides. Sections were fixed with 4% paraformaldehyde in PBS with overnight incubation. Apoptosis in the LV region of the mice heart was evaluated by terminal deoxynucleotidyl-transferase-mediated dUTP nick end labeling (TUNEL) assay (Roche Diagnostic, Penzberg, Germany) according to the manufacturer's instructions. Cardiomyocytes were differentiated by their localization within the myocardial tissue and by costaining with sarcomeric actin-α.

For the assessment of fibrosis, hearts were isolated and incubated overnight in 10% buffered formalin, embedded in paraffin, and sectioned serially at a thickness of 10 μM. Cross-sections of the ventricles were stained consecutively with Masson's Trichrome staining, followed by bright field imaging microscopy. Area of the heart sections stained in blue for collagen was considered as fibrotic area.

Echocardiography

In vivo heart function was assessed using a Vivid 7 ultrasound machine (GE Medical) equipped an il3L linear probe operated at 14 MHz. Mice were imaged in a conscious state at a room temperature of 73 °F and with decreased ambient lighting while held by an experienced handler in a supine left decubitus position. Mice were placed on an adjustable platform equipped with ECG electrodes to monitor heart and respiration rates. The heart was imaged in the 2-D mode in the parasternal long and short-axis views with a depth setting of 1.0 cm and at a frame rate of ≥275 frames/s. LV area was measured from short-axis views at papillary muscle levels, and an M-mode image was obtained at a sweep speed of 200 mm/s. Diastolic LV wall thickness, systolic LV wall thickness, LV end-diastolic dimension (LVEDD), and LV end-systolic chamber dimension (LVESD) were measured. All measurements were done from leading edge to leading edge according to American Society of Echocardiography guidelines. The percentage of LV SF was calculated as follows: SF =(LVEDD − LVESD)/LVEDD.

Isolation of Cardiomyocytes

Cardiomyocytes were isolated from mouse hearts as described previously.[8] Briefly, mice were anesthetized and the hearts were excised. Aorta was cannulated with a 20-guage needle and mounted on the perfusion apparatus. Perfusion solution was composed of Tyrodes buffer (150 mM NaCl, 10 mM dextrose, 5.4 mM KCl, 1.2 mM $MgCl_2$, 2 mM sodium pyruvate, and 5 mM HEPES), adding 5 mM taurine. Aorta was perfused for 2–3 min, and then 50 mg of type II collagenase (Invitrogen) and 6 mg of trypsin were added and perfused for 15 min. The temperature of the perfusate was maintained at 34 °C and all solutions were continuously bubbled with 95% O_2 and 5% CO_2. LV tissue was cleared of the heart vessels, atria, and the right ventricle and minced. Digested heart was filtered through 200 μm nylon mesh, placed in a conical tube, and centrifuged at 100 r.p.m. to allow viable cardiomyocytes

to settle. Supernatant was discarded and the cells were resuspended in MEM with Hank's salt and L-glutamine (HyClone, Thermo Scientific, Logan, UT, USA), with 10% fetal bovine serum, 100 units/ml penicillin, and 100 μg/ml streptomycin in a 5% CO_2 atmosphere at 37 °C. Cardiomyocyte cell death was determined using Trypan blue assay. Approximately 10–12 healthy cells per field from multiple mice were used for determining the cardiomyocyte area.

Western Blot Analysis

Western analyses were performed as described previously.[12] Briefly, whole-cell lysates were prepared using lysis buffer (50 mM Tris-HCl (pH =7.4), % Triton X-100, 150 mM NaCl, 1 mM EDTA, 2 mM Na_3VO_4, and 1 × Complete protease inhibitors (Roche)). The protein concentration was measured by the D_c protein assay (Bio-Rad). Densitometry of the bands was analyzed using NIH ImageJ software.

Statistical Analysis

Data analysis for animal model experiments was performed using GraphPad Prism 5.0 software. Significance was determined by ANOVA with Bonferroni post test. Effect of SB415286 on infarct size was analyzed using two-way ANOVA (P<0.05 was considered significant). For experiments *in vitro*, mean±s.d. were calculated from 3 to 4 independent experiments performed in quadruplicates. Student's two-tailed *t*-test was used to determine significant differences between treatment and control values.

RESULTS

Cardiac Structure Is Preserved in Akt1$^{-/-}$ Mice Following MI

In order to determine whether Akt1 is important for cardiac protection following MI, we induced MI in *Akt1*$^{+/+}$ and *Akt1*$^{-/-}$ mice by surgical ligation of the LAD coronary artery. TTC staining did not indicate any significant difference in infarct size between *Akt1*$^{+/+}$ and *Akt1*$^{-/-}$ hearts at 24 h after MI (P =0.85; Figure 1a and b). Interestingly, in an I/R injury model, infarct size in *Akt1*$^{-/-}$ hearts was 15% bigger compared with *Akt1*$^{+/+}$, but data were statistically not significant (Figure 1c and d). Thus, Akt1 signaling limits the cardiac damage after reperfusion but not after MI, showing differential role of Akt1. As GSK-3 is implicated in cardiac remodeling, we next determined whether GSK-3 inhibition would protect *Akt1*$^{-/-}$ hearts after I/R. Indeed, pretreatment with GSK-3 inhibitor (SB415286) significantly reduced the infarct size in *Akt1*$^{-/-}$ hearts compared with DMSO-treated controls (P<0.05; Figure 1c and d). However, pretreatment with SB415286 had no significant effect on the infarct size either between control (DMSO-treated) WT and *Akt1*$^{-/-}$ or between SB415286-treated WT and *Akt1*$^{-/-}$ hearts (Figure 1c and d). Evans blue perfusion showed no significant differences in the percentage of area at risk (AAR) between *Akt1*$^{+/+}$ and *Akt1*$^{-/-}$ hearts (Figure 1e). Together, these results indicate that although Akt1 deficiency does not exacerbate LV damage after an MI, Akt1 is necessary for cardioprotection following I/R injury via the Akt-1/GSK-3 axis.

GSK-3 Activation in Hearts of Akt1$^{-/-}$ Mice Leads to Enhanced Apoptosis Following MI

We first determined the effect of Akt1 deficiency in cardio-myocyte apoptosis at 24 h following MI. Our data indicated that *Akt1*$^{-/-}$ hearts exhibited increased numbers of TUNEL-positive cells compared with *Akt1*$^{+/+}$ hearts ($P<0.005$; Figure 2a). As GSK-3 activity increases in the absence of Akt1, we determined whether enhanced GSK-3 activity in *Akt1*$^{-/-}$ hearts had any effect on cardiomyocyte survival. As shown in Figure 2b, there were increased numbers of TUNEL-positive nuclei in the *Akt1*$^{-/-}$ hearts compared with *Akt1*$^{+/+}$ at 24 h after MI, and this effect was reduced by pretreatment with GSK-3α/β inhibitor SB415286. Quantification of the apoptotic nuclei in heart sections showed significantly enhanced apoptosis in *Akt1*$^{-/-}$ hearts compared with *Akt1*$^{+/+}$ ($P<0.05$; Figure 2c). Pretreatment with SB415286 significantly reduced apoptotic nuclei in both *Akt1*$^{+/+}$ ($P<0.05$) and *Akt1*$^{-/-}$ ($P<0.01$) hearts (Figure 2d). Thus, our results indicated that apoptosis is enhanced in *Akt1*$^{-/-}$ hearts as a result of increased GSK-3 activity, as GSK-3 inhibition reduced apoptosis in both *Akt1*$^{+/+}$ and *Akt1*$^{-/-}$ hearts to a similar level (Figure 2d).

In order to confirm that GSK-3 activity is increased in *Akt1*$^{-/-}$ mice hearts, we performed western analysis of *Akt1*$^{+/+}$ and *Akt1*$^{-/-}$ heart lysates treated with DMSO or SB415286 and collected 24 h after MI. Our data indicated that inhibitory serine-21/9 phosphorylation of GSK-3α/β by Akt1 was reduced in *Akt1*$^{-/-}$ hearts compared with *Akt1*$^{+/+}$ (Figure 2d). This, in turn, resulted in GSK-3 activation as evidenced by the changes in phosphorylation of β-catenin, a GSK-3 substrate (Figure 2d and e, left panel). As anticipated, effect of Akt1 deletion on GSK-3α/β phosphorylation (Figure 2d and e, right panel) and its activity ($P<0.02$) as evidenced by β-catenin phosphorylation (Figure 2d and e, left panel) was reversed ($P<0.001$) by pretreatment with SB415286.

Inhibition of GSK-3 Reverses Hypoxia-Induced Cell Death in Isolated Akt1$^{-/-}$ Mouse Cardiomyocytes

In order to assess the role of Akt1/GSK-3 signaling in cardiomyocyte survival, we determined the direct effects of hypoxia on the survival of isolated *Akt1*$^{+/+}$ and *Akt1*$^{-/-}$ cardiomyocytes. There were no significant differences in the survival of *Akt1*$^{+/+}$ and *Akt1*$^{-/-}$ cardiomyocytes under normoxic conditions. However, hypoxia (1% O_2) promoted cell death in cardiomyocytes and under these conditions, survival of *Akt1*$^{-/-}$ cardiomyocytes was dramatically reduced compared with *Akt1*$^{+/+}$ ($P<0.0001$; Figure 3a and b). We also observed that *Akt1*$^{-/-}$ cardio-myocytes were significantly smaller than the *Akt1*$^{+/+}$ cardiomyocytes (Figure 3c), further indicating a role for GSK-3 in the pathology ($P<0.02$). Pretreatment with SB415286 modestly, but significantly, reduced the cell death in *Akt1*$^{-/-}$ cardiomyocytes ($P<0.01$), indicating that enhanced apoptosis in *Akt1*$^{-/-}$ cardiomyocytes is, indeed, because of activation of GSK-3 (Figure 3d). Consistent with activation of GSK-3 and its role as an antihypertrophic molecule, myocytes from the *Akt1*$^{-/-}$ mice were smaller in size compared with *Akt1*$^{+/+}$. Together, these studies show that Akt/GSK-3 pathway is a critical regulator of cardiac myocyte signaling in response to hypoxia, supporting its role in cardiac ischemia.

Akt1 Deficiency Limits Post-MI Fibrosis and Enhances Survival Rate Following MI

Although we did not observe differences between *Akt1*$^{+/+}$ and *Akt1*$^{-/-}$ hearts 24 h after MI, we next assessed the consequences of Akt1 deletion on the long-term post-MI tissue remodeling such as fibrosis and on overall survival rate of the mice 4 weeks after MI. Masson's trichrome staining of the heart sections revealed 38% reduction in the fibrotic area (collagen staining) in *Akt1*$^{-/-}$ hearts compared with *Akt1*$^{+/+}$ ($P<0.02$; Figure 4a and b). As a result, there was a 25% reduction in the infarct size in *Akt1*$^{-/-}$ hearts compared with *Akt1*$^{+/+}$ hearts 4 weeks after MI ($P<0.05$; Figure 4c), despite the modest increase in cardiomyocyte apoptosis in *Akt1*$^{-/-}$ hearts compared with *Akt1*$^{+/+}$ 4 weeks after MI (Figure 4d; $P<0.05$). Consistently, although data were not significant, Kaplan–Meier survival curves showed that *Akt1*$^{-/-}$ mice may have better survival compared with *Akt1*$^{+/+}$ mice 4 weeks after MI as indicated by a trend toward statistical significance (Figure 4e), thus indicating that Akt1 deficiency protects against fibrosis and enhances overall survival following MI.

Akt1 Deficiency Leads to Improved Cardiac Function Following MI

We next determined the overall effect of Akt1 deficiency on cardiac function on day 4, week 2 and week 4 following MI. Even though impaired shortening fraction (SF) and ejection fraction (EF) were observed in *Akt1*$^{-/-}$ mice 24 h and 2 week after MI ($P<0.05$ and 0.01 for SF and $P<0.02$ and 0.05 for EF, respectively), both these parameters were improved in *Akt1*$^{-/-}$ mice 4 weeks after MI ($P<0.01$ for SF and $P<0.02$ for EF, respectively; Figure 5a and b), associated with a decrease in LV end-diastolic and systolic dimensions in ($P<0.03$ for LVEDd and $P<0.04$ LVESd, respectively) *Akt1*$^{-/-}$ mice as compared with *Akt1*$^{+/+}$ mice at 4 weeks after MI (Figure 5c and d). Our data indicated that in the long term, Akt1 deficiency preserves cardiac function following MI.

DISCUSSION

Although the importance of Akt1 in physiological cardiac hypertrophy has been previously reported,[13] multiple studies also point out that Akt1 is a critical mediator of pathological cardiac hypertrophy.[4–6] These conclusions, however, are derived from transgenic mouse models overexpressing constitutively active Akt1 at ~15-fold higher than the physiological levels. Overexpression of Akt1 to this extent can overtake the function of other Akt isoforms and also can lead to off-target effects because of nonphysiological protein–protein interactions and aberrant intracellular localization. Here, we show that Akt1 has dichotomous role in cardiac remodeling by mediating beneficial *versus* deleterious signaling based upon the duration and the type of stress. We demonstrate that Akt1 deficiency does not influence infarct size immediately after MI but exacerbates cardiac tissue damage and apoptosis of cardiomyocytes following reperfusion injury. This was also associated with decreased phosphorylation of GSK-3α/*β* and *β*-catenin. Enhanced apoptosis observed in *Akt1*$^{-/-}$ hearts *in vivo* after I/R and in *Akt1*$^{-/-}$ cardiomyocytes *in vitro* in response to hypoxia was reduced by pretreatment with the pan-GSK-3 inhibitor SB415286. A significant reduction in apoptosis with SB415286 was also observed in hearts. Interestingly, a more prominent consequence of Akt1 knockout in heart was diminished in cardiac fibrosis. This might contribute to improved cardiac function 4 weeks after MI in *Akt1*$^{-/-}$ hearts compared with *Akt1*$^{+/+}$. Altogether, our data demonstrate that the deficiency of Akt1 has differential

effects on short-term *vs* long-term consequences of MI and reperfusion injury. Although lack of Akt1 enhances LV damage and apoptosis in cardiomyocytes immediately after I/R injury, in a longer term, it improves cardiac function and LV remodeling after MI.

A key finding of our study is the utilization of GSK-3*β*/*β*-catenin pathway by Akt1 in the regulation of cardiomyocyte survival. Apart from this, our study demonstrates the net therapeutic effect of pan-GSK-3 inhibitor (SB415286) on the recovery of ischemic heart. A recent study has reported a paradoxical role for GSK-3α as compared with GSK-3*β* in cardiac ischemia.[9] Our data indicated that treatment with the pan-GSK-3 inhibitor overrides the role of GSK-3*α* to provide a net beneficial effect on improved ischemic recovery following MI. Detrimental effects of Akt1 deficiency on immediate tissue damage after I/R injury are reversed upon treatment with GSK-3 inhibitor SB415286. Similarly, a recent study by Woulfe *et al*[8] showed that deletion of GSK-3*β* in cardiomyocytes results in their enhanced proliferation and promotes protective effects on myocardium. Thus, it appears that inhibition of GSK-3*β* might serve as a potential strategy to minimize the pathological consequences immediately after MI. Such an idea is further supported by marked, yet similar, reductions in infarct size following pan-GSK-3 inhibition after I/R. However, the mechanisms by which GSK-3*β* activation in the absence of Akt1 leads to cardiomyocyte apoptosis and cardiac damage following an insult are not yet clear. It is likely that, in addition to apoptosis, GSK-3*β* activation induces autophagy in cardiomyocytes as has been recently reported.[14] As our data show that Akt1 deficiency is associated with enhanced GSK-3*β* activity and *β*-catenin phosphorylation, indicating that impaired Wnt signaling in cardiomyocytes may underlie the deleterious effects in the absence of Akt1.

The exact function of Wnt signaling, *β*-catenin in particular, in physiological and pathological cardiac hypertrophy remains controversial. Although downregulation of *β*-catenin has been reported to be necessary for adaptive cardiac remodeling,[15] recent studies indicate that *β*-catenin participates in augmenting cardiac hypertrophy[16] and postischemic cardiac remodeling[17] via activation of growth control genes.[18] Involvement of Akt in the modulation of Wnt signaling has been previously reported.[19] In this context, our data indicate that immediately after MI or I/R injury, enhanced GSK-3 activity in the absence of Akt1 results in increased phosphorylation and decreased stability of *β*-catenin, subsequently leading to its ubiquitination and proteolytic degradation. Enhanced postischemic cardiomyocyte apoptosis in *Akt1*$^{-/-}$ hearts is reversed upon GSK-3 inhibition and is associated with stabilization of *β*-catenin.

However, in the long term, Akt1 signaling seems to promote fibrosis in post-MI hearts. Akt1 function in cardiac fibrosis and hypertrophy is supported by multiple studies using both overexpression of Akt1 in heart[4,6] and Akt1 deletion[20] models and, therefore, less surprising. We have previously shown that Akt1 deficiency in mice results in impaired extracellular matrix assembly and remodeling in skin and blood vessels[2,3] because of impaired integrin activation[12] and impaired lamellipodia formation[21] in fibroblasts. In yet another model, Akt1/mTOR signaling is necessary for deposition of fibronectin and collagens by fibroblasts.[22] Most recently, our study demonstrated that sustained Akt1 activity in fibroblasts leads to its differentiation into pathological myofibroblasts via activation of a serum response factor transcription factor and myocardin pathway,

subsequently leading to enhanced collagen and fibronectin secretion.[23] Inhibition of Akt with triciribine was sufficient to reverse the TGFβ-induced myofibroblast differentiation and matrix protein secretion. In the current study, 4 weeks after MI, *Akt1*$^{-/-}$ hearts have less collagen deposition compared with *Akt1*$^{+/+}$, and this might make cardiac tissue more compliant to rapid postischemic remodeling processes. As a result of this, cardiac function was better preserved in *Akt1*$^{-/-}$ hearts 4 weeks after MI compared with *Akt1*$^{+/+}$ hearts, suggesting a unique pathological role for Akt1 contrary to its well-defined antiapoptotic role.

Taken together, this study clearly establishes Akt1/GSK-3 pathway as a key regulator of cardiomyocyte survival and remodeling of the ischemic heart. More importantly, these studies show the unique roles that Akt1 plays in regulating cardiac function on a short-term *versus* long-term basis, indicating the ability of Akt1 to integrate upstream signals to direct that downstream pathway. Critically, these data suggest that much more needs to be understood on the signaling consequences of Akt1 before developing novel therapeutic strategies. Thus, targeting both Akt1 and GSK-3 pathways needs to be considered to diminish the detrimental consequences of ischemic heart diseases.

Acknowledgments

We acknowledge the funds provided by the National Institutes of Health: HL103952 to PRS and HL071625 to TVB.

References

1. Somanath PR, Razorenova OV, Chen J, Byzova TV. Akt1 in endothelial cell and angiogenesis. Cell Cycle. 2006; 5:512–518. [PubMed: 16552185]
2. Chen J, Somanath PR, Razorenova O, Chen WS, Hay N, Bornstein P, et al. Akt1 regulates pathological angiogenesis, vascular maturation and permeability in vivo. Nat Med. 2005; 11:1188–1196. [PubMed: 16227992]
3. Somanath PR, Chen J, Byzova TV. Akt1 is necessary for the vascular maturation and angiogenesis during cutaneous wound healing. Angiogenesis. 2008; 11:277–288. [PubMed: 18415691]
4. Shiojima I, Sato K, Izumiya Y, Schiekofer S, Ito M, Liao R, et al. Disruption of coordinated cardiac hypertrophy and angiogenesis contributes to the transition to heart failure. J Clin Invest. 2005; 115:2108–2118. [PubMed: 16075055]
5. Shiojima I, Walsh K. Regulation of cardiac growth and coronary angiogenesis by the Akt/PKB signaling pathway. Genes Dev. 2006; 20:3347–3365. [PubMed: 17182864]
6. Nagoshi T, Matsui T, Aoyama T, Leri A, Anversa P, Li L, et al. PI3K rescues the detrimental effects of chronic Akt activation in the heart during ischemia/reperfusion injury. J Clin Invest. 2005; 115:2128–2138. [PubMed: 16007268]
7. Sugden PH, Fuller SJ, Weiss SC, Clerk A. Glycogen synthase kinase 3 (GSK3) in the heart: a point of integration in hypertrophic signalling and a therapeutic target? A critical analysis. Br J Pharmacol. 2008; 153(Suppl 1):S137–S153. [PubMed: 18204489]
8. Woulfe KC, Gao E, Lal H, Harris D, Fan Q, Vagnozzi R, et al. Glycogen synthase kinase-3beta regulates post-myocardial infarction remodeling and stress-induced cardiomyocyte proliferation in vivo. Circ Res. 2010; 106:1635–1645. [PubMed: 20360256]
9. Lal H, Zhou J, Ahmad F, Zaka R, Vagnozzi RJ, Decaul M, et al. Glycogen synthase kinase-3alpha limits ischemic injury, cardiac rupture, post-myocardial infarction remodeling and death. Circulation. 2012; 125:65–75. [PubMed: 22086876]

10. Cai ZP, Shen Z, Van Kaer L, Becker LC. Ischemic preconditioning-induced cardioprotection is lost in mice with immunoproteasome subunit low molecular mass polypeptide-2 deficiency. Faseb J. 2008; 22:4248–4257. [PubMed: 18728217]
11. Gross ER, Hsu AK, Gross GJ. Opioid-induced cardioprotection occurs via glycogen synthase kinase beta inhibition during reperfusion in intact rat hearts. Circ Res. 2004; 94:960–966. [PubMed: 14976126]
12. Somanath PR, Kandel ES, Hay N, Byzova TV. Akt1 signaling regulates integrin activation, matrix recognition, and fibronectin assembly. J Biol Chem. 2007; 282:22964–22976. [PubMed: 17562714]
13. DeBosch B, Treskov I, Lupu TS, Weinheimer C, Kovacs A, Courtois M, et al. Akt1 is required for physiological cardiac growth. Circulation. 2006; 113:2097–2104. [PubMed: 16636172]
14. Zhai P, Sadoshima J. Glycogen synthase kinase-3beta controls autophagy during myocardial ischemia and reperfusion. Autophagy. 2012; 8:138–139. [PubMed: 22113201]
15. Baurand A, Zelarayan L, Betney R, Gehrke C, Dunger S, Noack C, et al. Beta-catenin downregulation is required for adaptive cardiac remodeling. Circ Res. 2007; 100:1353–1362. [PubMed: 17413044]
16. Hahn JY, Cho HJ, Bae JW, Yuk HS, Kim KI, Park KW, et al. Beta-catenin overexpression reduces myocardial infarct size through differential effects on cardiomyocytes and cardiac fibroblasts. J Biol Chem. 2006; 281:30979–30989. [PubMed: 16920707]
17. Zelarayan LC, Noack C, Sekkali B, Kmecova J, Gehrke C, Renger A, et al. Beta-Catenin downregulation attenuates ischemic cardiac remodeling through enhanced resident precursor cell differentiation. Proc Nat Acad Sci USA. 2008; 105:19762–19767. [PubMed: 19073933]
18. Armstrong DD, Esser KA. Wnt/beta-catenin signaling activates growth-control genes during overload-induced skeletal muscle hypertrophy. Am J Physiol. 2005; 289:C853–C859.
19. Fukumoto S, Hsieh CM, Maemura K, Layne MD, Yet SF, Lee KH, et al. Akt participation in the Wnt signaling pathway through Dishevelled. J Biol Chem. 2001; 276:17479–17483. [PubMed: 11278246]
20. Shimizu I, Minamino T, Toko H, Okada S, Ikeda H, Yasuda N, et al. Excessive cardiac insulin signaling exacerbates systolic dysfunction induced by pressure overload in rodents. J Clin Invest. 2010; 120:1506–1514. [PubMed: 20407209]
21. Somanath PR, Byzova TV. 14-3-3beta-Rac1-p21 activated kinase signaling regulates Akt1-mediated cytoskeletal organization, lamelli-podia formation and fibronectin matrix assembly. J Cell Physiol. 2009; 218:394–404. [PubMed: 18853424]
22. Goc A, Choudhary M, Byzova TV, Somanath PR. TGFbeta- and bleomycin-induced extracellular matrix synthesis is mediated through Akt and mammalian target of rapamycin (mTOR). J Cell Physiol. 2011; 226:3004–3013. [PubMed: 21302298]
23. Abdalla M, Goc A, Segar L, Somanath PR. Akt1 mediates alpha-smooth muscle actin expression and myofibroblast differentiation *via* myocardin and serum response factor. J Biol Chem. 2013; 288:33483–33493. [PubMed: 24106278]

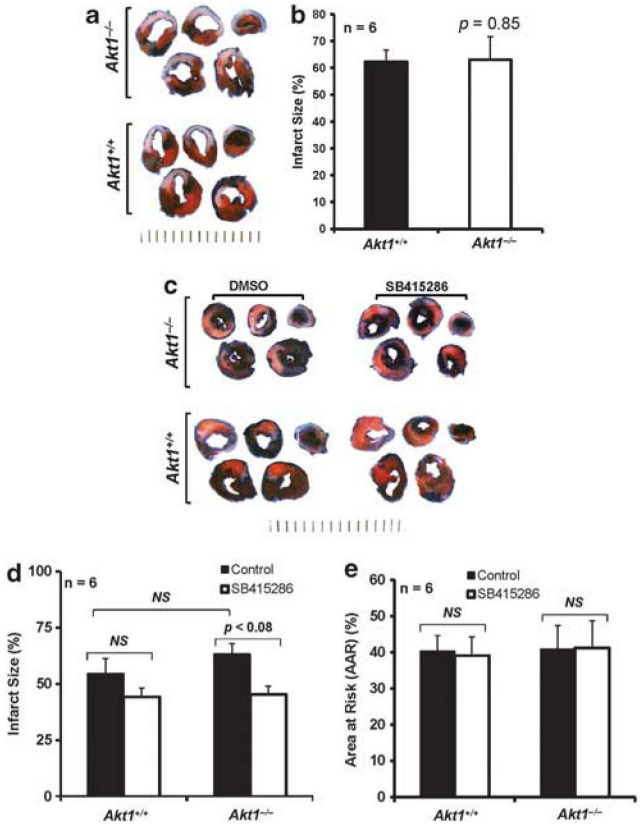

Figure 1.

Cardiac structure is preserved in *Akt1*$^{-/-}$ mice after MI. (**a**) Representative images of the *Akt1*$^{+/+}$ and *Akt1*$^{-/-}$ mice heart sections taken at 24 h after permanent occlusion of the LAD artery and stained with 2,3,5-triphenyltetrazolium chloride (TTC). (**b**) Quantification of the infarct area in *Akt1*$^{+/+}$ and *Akt1*$^{-/-}$ mice hearts represented as mean ±s.e.m., indicating no difference in infarct area between *Akt1*$^{+/+}$ and *Akt1*$^{-/-}$ mice. (**c**) Representative images of the TTC-stained heart sections taken at 24 h after cardiac I/R in the presence of DMSO or GSK-3 inhibitor SB415286 showing bigger infarct area in *Akt1*$^{-/-}$ hearts compared with *Akt1*$^{+/+}$ and reversal of this effect upon pretreatment with GSK-3 inhibitor SB415286. (**d**) Quantification of the infarct area in *Akt1*$^{+/+}$ and *Akt1*$^{-/-}$ mice hearts in the presence of DMSO or SB415286 represented as mean percentage infarcted ±s.e.m. (**e**), Bar graph indicating no difference in the area at risk (AAR; mean percentage± s.e.m.) between *Akt1*$^{+/+}$ and *Akt1*$^{-/-}$ mice hearts demonstrating that the level of occlusion of LAD is similar in both groups (*n* =6/group).

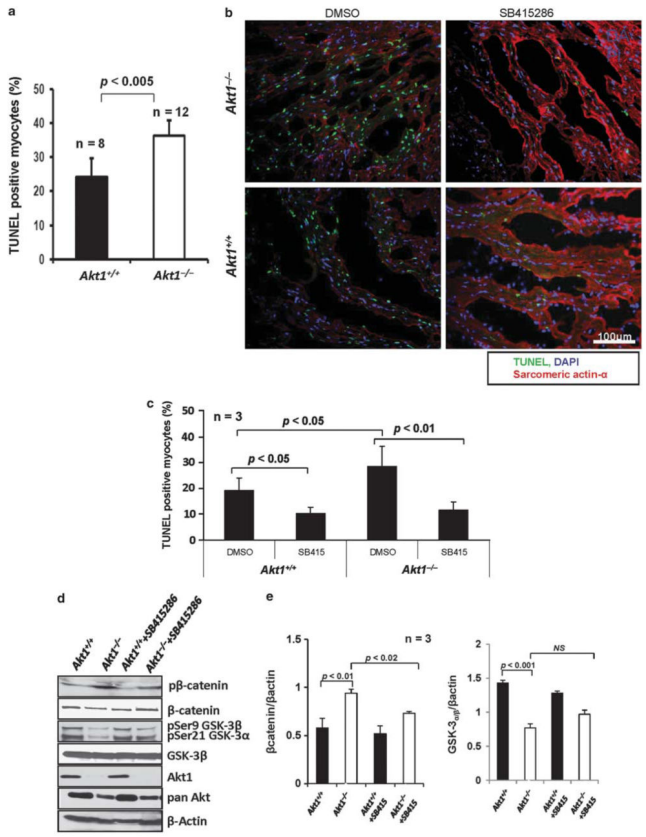

Figure 2.

Enhanced apoptosis in *Akt1*$^{-/-}$ mice hearts following MI is reversed by GSK-3 inhibition. (**a**) Quantification of the TUNEL-positive cells in *Akt1*$^{+/+}$ and *Akt1*$^{-/-}$ mice hearts 24 h after MI (n =8–12) represented as mean apoptotic area±s.e.m., indicating significantly higher number of apoptotic cells in *Akt1*$^{-/-}$ hearts compared with *Akt1*$^{+/+}$. (**b**) Representative TUNEL (green) staining images of the heart *Akt1*$^{+/+}$ and *Akt1*$^{-/-}$ heart sections taken at 24 h after MI in the presence of DMSO or SB415286. Sarcomeric actin-α (red) and nuclei (DAPI, blue) demonstrate morphology. (**c**) Quantification of the TUNEL-positive cells in *Akt1*$^{+/+}$ and *Akt1*$^{-/-}$ mice hearts at 24 h after -MI represented as mean apoptotic area±s.e.m., indicating that pretreatment with SB415286 significantly inhibited apoptosis in *Akt1*$^{+/+}$ and *Akt1*$^{-/-}$ hearts (n =3/group). (**d**) Western blots of *Akt1*$^{+/+}$ and *Akt1*$^{-/-}$ heart lysates collected at 24 h after MI in the presence of DMSO or SB415286 showing changes in GSK-3 activity as evidenced by changes in β-catenin phosphorylation. (**e**) Band densitometry analysis of the western blots of *Akt1*$^{+/+}$ and *Akt1*$^{-/-}$ heart lysates revealing changes in the phosphorylation of GSK-3α/β (right panel) and β-catenin (left panel) normalized to loading control β-actin, collected at 24 h after MI in the presence of DMSO or SB415286.

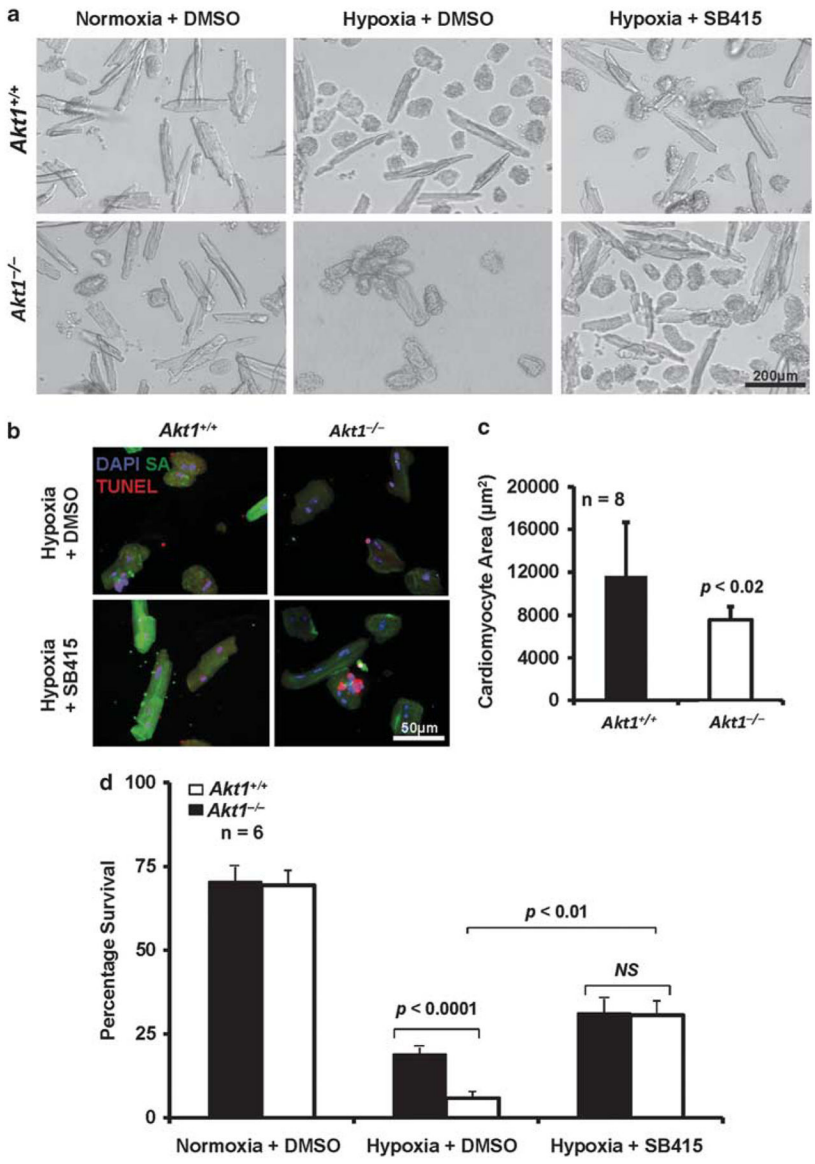

Figure 3.

Hypoxia-induced cardiomyocyte death in *Akt1*$^{-/-}$ mice is reversed by GSK-3 inhibition. (**a**, **b**) Representative images of the *Akt1*$^{-/-}$ and *Akt1*$^{+/+}$ cardiomyocytes (**a**, phase contrast and **b**, TUNEL stained in red) taken after 2 h of hypoxia *in vitro*. (**c**) Bar graph showing significantly smaller size of *Akt1*$^{-/-}$ cardiomyocytes compared with *Akt1*$^{+/+}$ (*n* =8/group) after hypoxia treatment. (**d**) Quantification of the viability of *Akt1*$^{+/+}$ and *Akt1*$^{-/-}$ mouse cardiomyocytes after hypoxia pretreated with vehicle control (DMSO) or SB415286 represented as mean percentage survival±s.e.m. indicating significantly enhanced cell death in the absence of Akt1(*n* =6/group).

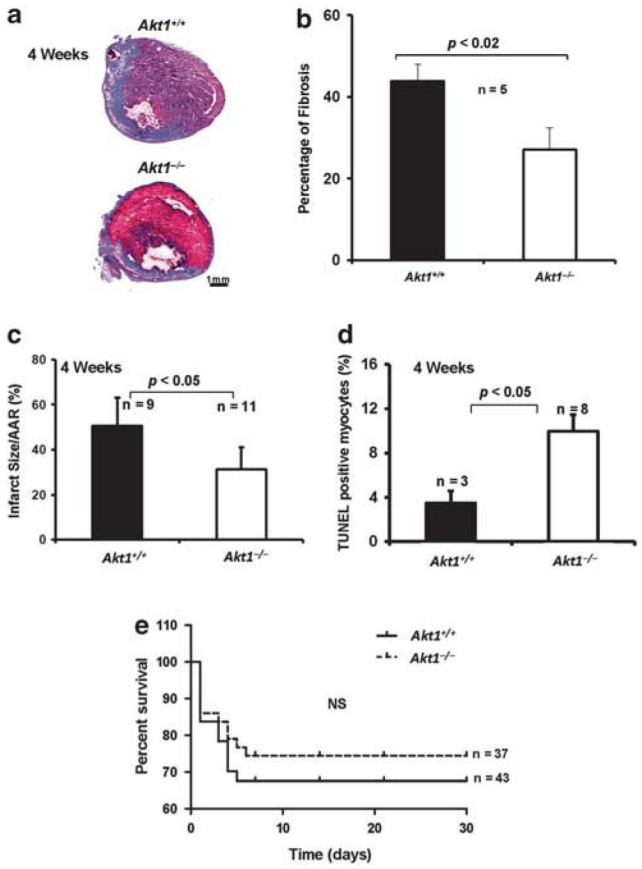

Figure 4.

Improved cardiac remodeling and enhanced survival rate in *Akt1*$^{-/-}$ mice 4 weeks after MI. (**a**) Representative images of the *Akt1*$^{+/+}$ and *Akt1*$^{-/-}$ mice heart sections stained with Masson's trichrome staining showing fibrosis 4 weeks after MI. (**b**) Quantification of the fibrotic area in mice hearts represented as mean percentage of fibrosis±s.e.m. indicating significantly larger fibrotic area 4 weeks after MI in *Akt1*$^{+/+}$ hearts compared with *Akt1*$^{-/-}$ hearts (n =5/group). (**c**) Quantification of the infarct area in *Akt1*$^{+/+}$ and *Akt1*$^{-/-}$ mice hearts 4 weeks after MI represented as mean±s.e.m., indicating significantly lesser infarct area in *Akt1*$^{-/-}$ mice compared with *Akt1*$^{+/+}$ mice (n =9–11). (**d**) Quantification of the TUNEL-positive cells in *Akt1*$^{+/+}$ and *Akt1*$^{-/-}$ mice hearts 4 weeks after MI (n =3–8) represented as mean apoptotic area±s.e.m. indicating significantly higher number of apoptotic cells in *Akt1*$^{-/-}$ hearts compared with *Akt1*$^{+/+}$. (**e**) *Akt1*$^{+/+}$ and *Akt1*$^{-/-}$ mice were subjected to MI or sham surgery and survival was monitored for 30 days and analyzed by the Kaplan–Meier method (n =37 and 43).

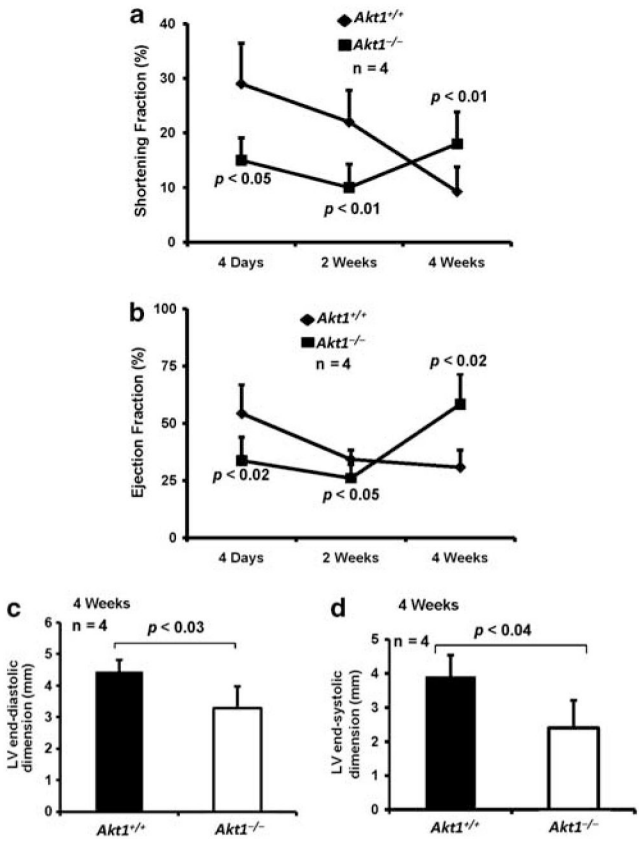

Figure 5.

Cardiac function is preserved in *Akt1*$^{-/-}$ mice 4 weeks after MI. (**a**) Figure showing improved shortening fraction (FS) in *Akt1*$^{-/-}$ mice hearts at 4 days, 2 weeks, and 4 weeks after MI compared with *Akt1*$^{+/+}$ hearts (*n* =5/group). (**b**) Figure showing improved ejection fraction (EF) in *Akt1*$^{-/-}$ mice hearts at 4 days, 2 weeks, and 4 weeks after MI compared with *Akt1*$^{+/+}$ hearts (*n* =5/group). (**c**) Bar graph showing reduced LV end-diastolic dimension in *Akt1*$^{-/-}$ hearts compared with *Akt1*$^{+/+}$ hearts (*n* =4/group). (**d**) Bar graph showing reduced LV end-systolic dimension in *Akt1*$^{-/-}$ hearts compared with *Akt1*$^{+/+}$ hearts (*n* =4/group).